TURNING ANGLES ON CONVEX IDEAL HYPERBOLIC POLYHEDRA

SEBASTIAN CALVO

ABSTRACT. The aim of the paper is to provide insight on polygonal curves in hyperbolic 3-space. We will focus on a particular class of closed curves, namely closed simple-sequence curves on convex ideal polyhedra. First, given such a path, we glue the visited faces to find a Möbius map, which will determine if there is a closed geodesic representative in its isotopy class. Then we expand on Igor Rivin's inequality surrounding turning and dihedral angles and construct an explicit equality for closed polygonal curves on convex hyperbolic polyhedra. Finally, we demonstrate an example to showcase the techniques and findings discussed in this paper.

CONTENTS

1. INTRODUCTION

Hyperbolic space captures a vibrant and very much distinct geometry from Euclidean space. Igor Rivin has done significant work in the field by characterizing polyhedra in hyperbolic 3-space **[2],[3]**. A property of an ideal convex polyhedron that reveals to be an underpin to the structure of the polyhedron is the dihedral angles of the polyhedron. Using dihedral angles, Rivin was able to construct an upper bound of the turning angle of a polygonal segment. I studied Rivin's upper bound for the turning angle, and investigated under what conditions would this inequality become an equality.

2. BACKGROUND

The following background material is excerpted from [1]. For $a, b, c, d \in \mathbb{C}$, define a *Möbius transformation* $A : \overline{\mathbb{C}} \to \overline{\mathbb{C}}$ by $z \mapsto \frac{az+b}{cz+d}$ where $\overline{\mathbb{C}} = \mathbb{C} \cup \{\infty\}$ and $ad - bc \neq 0$. The set of Möbius transformations Σ has a correspondence with $PSL(2, \mathbb{C})$, that is for $A(z) = \frac{az+b}{cz+d}$, $A(z) \sim A$ where $A = \begin{bmatrix} a & b \\ c & d \end{bmatrix} \in PSL(2, \mathbb{C})$. Möbius transformations are conformal orientation-preserving automorphisms of $\overline{\mathbb{C}}$. Another neat property of these maps that will be useful to us is they send circles & lines to circles & lines.

Given distinct z_1, z_2, z_3 points of $\overline{\mathbb{C}}$, there is a unique Möbius map that takes them to $1, 0, \infty$ respectively called the *cross-ratio* defined as

$$C : z \mapsto \frac{(z - z_2)(z_1 - z_3)}{(z - z_3)(z_1 - z_2)} = (z, z_1, z_2, z_3)$$

Using the cross-ratio, we can argue the following proposition.

Proposition 2.1 The group Σ acts 3-transitively on $\overline{\mathbb{C}}$.

Proof: Suppose we have the pair of three coordinates $P = \{p_1, p_2, p_3\}$ and $Q = \{q_1, q_2, q_3\}$, where $p_i, q_i \in \overline{\mathbb{C}}$ and each element p_i, q_i is distinct in its corresponding set. Then consider the cross-ratios (z, p_1, p_2, p_3) and (z, q_1, q_2, q_3). Since the cross-ratio corresponding to Q is bijective, it has a unique inverse. This unique inverse is of the form

$$Q^{-1}(z) = \frac{(q_1q_3 - q_2q_3)z + q_2q_3 - q_1q_2}{(q_1 - q_2)z + q_3 - q_1}$$

This inverse map sends $1 \mapsto q_1, 0 \mapsto q_2$ and $\infty \mapsto q_3$, while the cross-ratio $P(z)$ corresponding to P sends $p_1 \mapsto 1, p_2 \mapsto 0$ and $p_3 \mapsto \infty$. Then by composing $Q^{-1} \circ P(z)$, we obtain a map that sends $p_i \mapsto q_i$. Thus Σ acts 3-transitively on $\overline{\mathbb{C}}$. $\square$

We can rephrase the previous proposition to state that a Möbius transformation is uniquely determined by what it does to 3 points. For $A, B \in PSL(2, \mathbb{C})$, A is *conjugate* to B if there exists a $U \in PSL(2, \mathbb{C})$ such that $UAU^{-1} = B$. There are 3 classes of Möbius maps which are defined as follows.

A is *parabolic* if
- the trace of A is ± 2
- A is conjugate to a translation and fixes only infinity

A is *elliptic* if
- the trace of A is real in $(-2, 2)$
- A is conjugate to a rotation that fixes 0 and infinity

A is *loxodromic* if
- the trace of A is in $\mathbb{C}\backslash[-2, 2]$
- A is conjugate to a map B and B is of form $\begin{bmatrix} \lambda & 0 \\ 0 & 1/\lambda \end{bmatrix}$ where $|\lambda| \neq 1$
- A has 2 fixed points where one acts as a repelling point and the other acts an attracting point

The two models for $\mathbb{H}^2$ we emphasize are the *upper-half plane* and the *disk* models. The upper-half plane model is defined as $\{z \in \mathbb{C} | \ \mathrm{Im}(z) > 0\} \cup \{\infty\}$ and the disk model is defined as $\{z \mid |z| < 1, z \in \mathbb{C}\}$. The metrics are distinct from the Euclidean metric. For example, the norm of a vector in the upper-half plane is defined as $\frac{|.|_e}{y}$ where $|.|_e$ is the Euclidean metric and y is the imaginary component. The geodesics in each model are lines orthogonal to the boundary, where the boundary is the real line for the former and S^1 for the latter. Let $q(x, y)$ denote the geodesic containing x and y. For the upper-half plane, we will call the two types of geodesics *vertical* and

bowed. The two models are equivalent, that is, we can use a Möbius map, $U(z) = \frac{z+i}{iz+1}$ for example, to go from one to the other. The group Σ is interesting to us because in fact the subgroup $PSL(2,\mathbb{R})$ are isometries for the upper-half plane.

The beauty of Möbius maps is that Σ extends naturally when we consider $\mathbb{H}^3$, as do the upper-half plane and disk models. For $\mathbb{H}^3$, we can naturally produce the *upper-half space* and *ball* model. The upper-half space is defined as $\{(z,t)|z \in \mathbb{C},\ t \in \mathbb{R}, t > 0\}$. The geodesics of these models are Euclidean planes or sections of spheres orthogonal to the boundaries $\mathbb{C}$ and S^2 respectively. Analogously, we can go from one to the other by a Möbius map as well as the metric for the upper-half space is the euclidean metric equipped with a scaling factor corresponding to the third coordinate. The metric for the ball model is $ds = \frac{2|d\vec{x}|}{1-|\vec{x}^2|}$.

3. Polygonal Curves

Let us now briefly discuss definitions and overall ideas. The following is found in **[3]**.

Definition 3.1 Let γ be a curve. We say γ is *polygonal* if its piece-wise components are geodesics where end points of geodesics are vertices of γ.

Definition 3.2 Let γ be a closed polygonal curve in $\mathbb{H}^3$, with vertices $p_1, ..., p_{k-1}, p_k = p_1$. Then we define the *turning angle* $\tau_i(\gamma)$ of γ at the vertex p_i to be the exterior angle of triangle $T_i = p_{i-1}p_ip_{i+1}$ at p_i, and define the *total turning angle* $\tau(\gamma)$ of γ to be $\sum_{i=1}^{k} \tau_i(\gamma)$. (Notice $\tau(\gamma) = 0$ if and only if γ is a geodesic.)

These definitions make sense in whichever metric space we are established in. However since we are focused on hyperbolic geodesics, the piece-wise components will be segments of either vertical or bowed geodesics. The closed polygonal curves we will be interested in are those that lie on the faces of a convex ideal polyhedron P in $\mathbb{H}^3$. The following is an example of our interest.

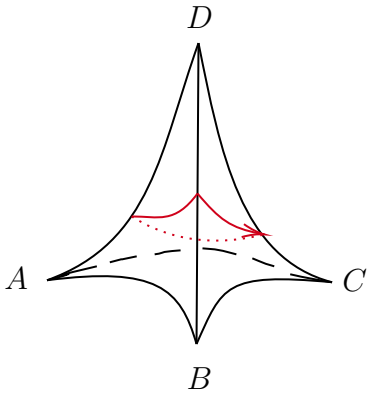

Since P is 2-manifold, then we can treat each face of P is a copy of $\mathbb{H}^2$. That is, the polyhedron is locally isometric to $\mathbb{H}^2$ except at its ideal vertices. Recall that since we do not consider the boundary of $\mathbb{H}^3$ as part of the space, a polygonal curve is not allowed to pass through a polyhedron's ideal vertex. Thus along an edge of the polyhedron is fair game for a polygonal curve to pass through. In fact, if the curve passes through an edge, then one can think of the edge as the gluing of two copies of $\mathbb{H}^2$ along the geodesic that contains said edge. We end this section with a theorem and

a lemma discussed by Rivin that will be the stepping stone of our investigation [3, 84].

Theorem 3.3 (Hyberbolic Fenchel Theorem) The total turning of a closed polygonal curve γ in $\mathbb{H}^3$ is greater than 2π, unless all of the vertices are collinear.

Lemma 3.4 Let H_1 and H_2 be two geodesic half-planes meeting at a dihedral angle α, and γ_1, γ_2 geodesic segments on H_1, H_2 respectively meeting at a point p on $H_1 \cap H_2$. If $\gamma = \gamma_1 \cup \gamma_2$ is a geodesic in the intrinsic metric on $H_1 \cup H_2$, then the turning angle $\tau_p(\gamma)$ is no larger than the exterior dihedral angle $\pi - \alpha$ at $H_1 \cap H_2$.

4. The parabolic case

To realize a face F of P as a copy of $\mathbb{H}^2$, consider the geodesic plane G that F is a subset of. Suppose we have our polyhedron P in upper-half space. Considering If G is a Euclidean plane orthogonal to boundary, we treat the surface as an upper-half plane which we then could translate to a disk model. If G is a spherical plane orthogonal to the boundary, a stereographic projection of G onto the boundary gives a copy of a disk model. Since $F \subset G$, the copy of disk model will obtain a geodesic for each corresponding edge of F as well as a finite set of vertices on the boundary of $\mathbb{H}^2$.

Consider a closed curve γ on a convex polyhedron P in $\mathbb{H}^3$ whose *face sequence is basic*, that is, an oriented γ passes through faces γ enters & exits a face only once. Figure 1 is an example of a curve γ whose face sequence is basic. Notice how we aren't yet restricting γ to be polygonal. In other words, the curve may not locally look like a hyperbolic geodesic. Given this parameter, the question we aim to answer is could we construct a closed polygonal curve that mimics the face sequence of γ *and* adopts a more explicit relationship between angles than Lemma 3.3 presents. This approach leads us to a neat distinction between classes of curves γ: those that strictly go around a single vertex of P and those that don't. Let us discuss about the former first.

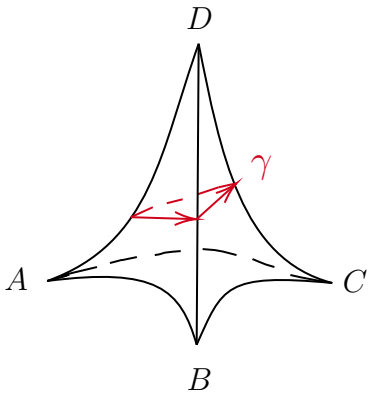

Figure 1

To illustrate this distinction, let P again be the hyperbolic tetrahedron and γ be a closed curve as shown above. As mentioned previously, since we can realize each face

as a copy of $\mathbb{H}^2$, the copies of $\mathbb{H}^2$ will capture the components of γ that lie in their respective faces.

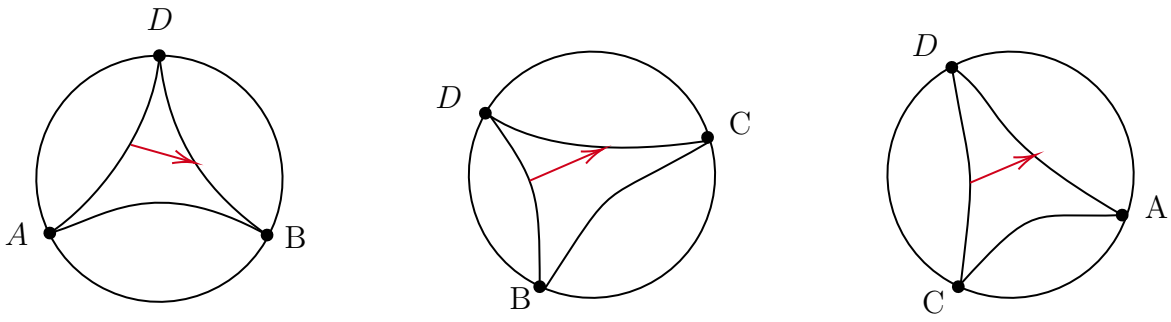

FIGURE 2. Faces $(ABD), (CBD)$ and (ACD) of P as disjoint copies of $\mathbb{H}^2$

Being able to drop down a dimension in hyperbolic space is neat because $\mathbb{H}^2$ is computationally friendlier than in $\mathbb{H}^3$. Recall along an edge in $\mathbb{H}^3$, there is an instricic metric on $H_1 \cup H_2$. This same idea translates to one dimension lower. If two faces F_1 and F_2 are joined along a geodesic, we can obtain a metric such between the two. To obtain such a scenario, we must first topologically cut and paste the 2 polygonal faces along the geodesic edges that separate them. If we didn't think Möbius maps were special enough, we can once again praise their remarkable characteristics as the gluing maps we will be using are in fact elements of Σ.

Let us now think about the gluing process. It is not enough to glue faces of $\mathbb{H}^2$ along the geodesic that separates them simply by identifying their ideal vertices. Why is this? Recall that Möbius maps take geodesics to geodesics. But Möbius maps are uniquely determined by what it does to 3 points, so if we only choose to identify corresponding vertices, then we will family of infinitely acceptable maps that do this. Which one would we choose? As our curve γ is passing from one face to another, there is only a single point on the edge between them that γ passes through. From our family of acceptable gluing maps, we choose the unique map that identifies the 'exiting' point of the first face with the 'entering' point of the second. Let's see what this means for our faces above in Figure 2.

These copies of $\mathbb{H}^2$ are disjoint but notice we are identifying vertices of these disjoint copies by the same letter. This manner of identifying them is valid after all we are simply recognizing the ideal vertices of P. This lends itself to be a double-edged sword because of our multitude of the same letter in these *disjoint* copies, notation can quickly become chaotic. Thus let us rename our variables neatly.

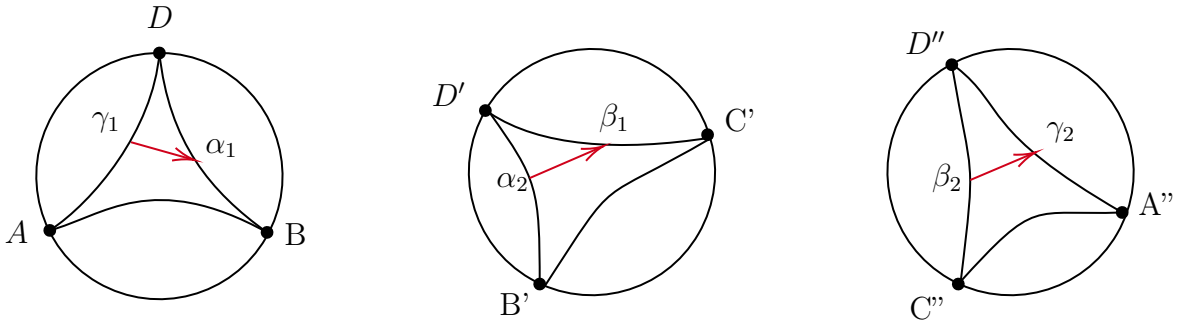

Using the fact that 3 assignments determine a Möbius map, we can now clearly construct our gluing maps. The way we will be gluing our faces together is by gluing every face in sequential order onto the first face, which in our example is the face (ABD). Once we glue the second face onto the first face, we glue the third face onto the first, which has the gluing of second face already applied.

$$g_1(z) : D' \mapsto D, B' \mapsto B, \alpha_2 \mapsto \alpha_1$$

$$g_2(z) : D'' \mapsto D, C'' \mapsto g_1(C'), \beta_2 \mapsto g_1(\beta_1)$$

When we apply our gluing maps, we have the following resulting presentation of the faces γ lives on.

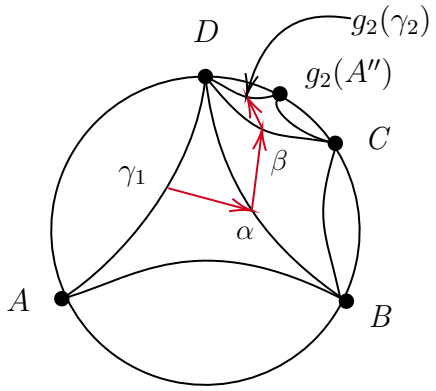

Our curve γ had the property that it went around a single vertex of P. This property is also easily visualized in our realization of γ onto $\mathbb{H}^2$, as all the faces have the vertex in question. To assure that our curve is closed in $\mathbb{H}^2$, our final gluing map will be the map that fixes D, maps A to $g_2(A'')$ and γ_1 to $g_2(\gamma_2)$. We are now in a position to assert our first finding in our investigation.

Theorem 4.1 For a closed curve γ whose face sequence is basic and goes around a single vertex v of an ideal hyperbolic polyhedron, the final gluing map is a parabolic Möbius transformation.

Proof: Arbitrarily choose an edge e that contains v and call either face the edge borders the first face, which we will denote F_1. Call the other face F_k. This along with the fact that γ goes around v determines a sequential order of n faces, all of which contain v both in $\mathbb{H}^3$ and in the realization of the faces γ lives on in $\mathbb{H}^2$. Because γ is

closed, the face sequence must come back to the arbitrarily chosen edge e to maintain γ's closed condition. Thus in the realization of γ in $\mathbb{H}^2$, the curve will start at e at a point γ_1, progress and then eventually hit e at a point γ_2. Let w be the other vertex of e. Then construct the unique map φ that fixes v, sends w to $g_{n-1}(w^{(n-1)})$ and γ_1 to $g_{n-1}(\gamma_2)$. The picture we should have in our heads is the following, with the ... signifying the edges inbetween that also contain v.

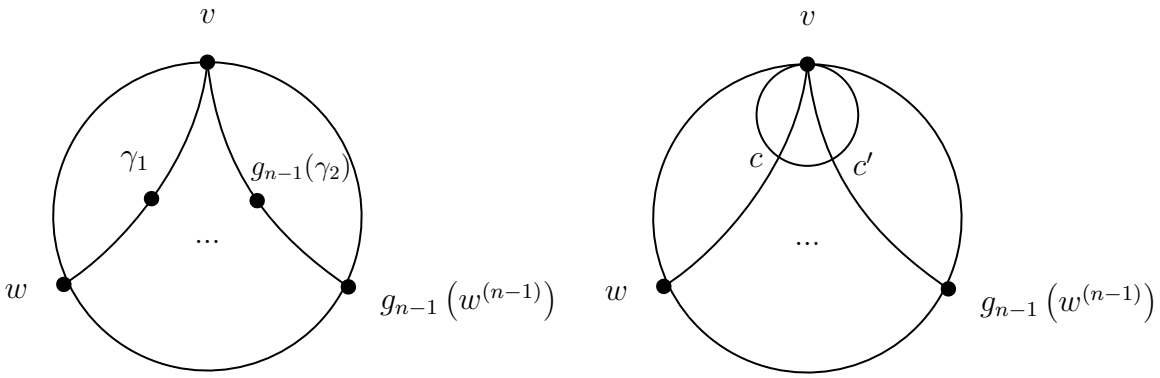

FIGURE 3. The picture we should have in our heads (left) and horocircle realization (right)

In order to continue, I should comment about the following idea we will be using. The face sequence of γ is more important than γ itself. The main reason we use γ is to help us identify edge points so that our gluing becomes intuitive and straightforward. If however, a curve $\overline{\gamma}$ followed the same face sequence as γ on the same polyhedron P but glued along different edge points, then the topological gluing of $\overline{\gamma}$ will be the same as γ by the principle that the edge point on the edge doesn't matter.

Consider a horosphere at v in $\mathbb{H}^3$ that intersects the faces around v such that the realization of $\mathbb{H}^2$ contains a horocircle $\mathcal{C}$ at v, as shown above. At this point, we are abandoning γ and choosing the curve $\overline{\gamma}$ along $\mathcal{C}$ from c to c' where $c = \mathcal{C} \cap q(v, w)$ and $c' = \mathcal{C} \cap q(v, g_{n-1}(w^{(n-1)}))$ as in the figure above. We are likewise constructing a new map $\overline{\varphi}$ that fixes v, sends w to $g_{n-1}(w^{(n-1)})$ but now takes c to c'. To make the upshot more transparent, let's translate the disk model to the upper-half plane, sending v to ∞ and identifying w with x.

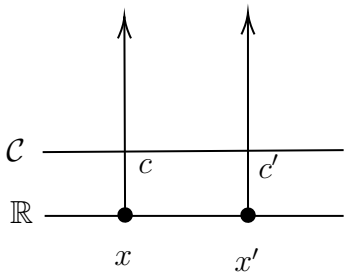

The horocircle C must be parallel to the real line, since it was only tangent to the boundary of S^1 in the disk model. The map $\overline{\varphi}$ is clearly a translation and thus it is a parabolic Möbius map. $\square$.

5. The Loxodromic case

We saw that for a basic curve going around a vertex of an ideal polyhedron results in a corresponding parabolic map. Now let us think about curves that do not go around a vertex– these will correspond to a loxodromic map. We are actually more interested in the loxodromic case; the parabolic case was just a neat sidetrack. But instead of following along the construction process for the parabolic case. Let us get right to the point.

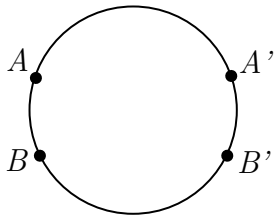

Figure 4. The set up for a corresponding loxodromic map

For a curve γ that doesn't go around a vertex, we will have the picture above. We can quickly convince ourselves of this by noticing since there is no fixed vertex, γ must pass through at least one edge that doesn't share vertices with some other edge. The said picture contains the points of the principal pair of points and terminal pair of points, where by 'principal' we mean the edge where γ starts and by 'terminal' we mean the edge where γ terminates. We should remember that by doing the gluing construction as done in the parabolic case, we will obtain more ideal vertices, geodesic edges and polygonal faces but we are currently choosing to not focus on those yet. Let us know show a barrage of facts about Figure 4.

Proposition 5.1 Given the $\mathbb{H}^2$ realization of γ as in Figure 4, the corresponding gluing map is loxodromic.

Proof: We prove this by cases. First suppose the gluing map φ is parabolic. Denote $\widehat{xy}$ to be the shortest arc of S^1 determined by x and y.

> Case 1: Suppose the fixed point of φ is in $\widehat{AA'}$. Then since φ since is parabolic, that means it simply rotates along the boundary. So $q(A, B)$ is rotated to $q(A', B')$ in counterclockwise orientation but B was supposed to be to the right of A, whereas B' is to the left of A'. Since φ swapped orientation, this case fails.
>
> Case 2: Suppose the fixed point of φ is in $\widehat{BB'}$. This case is analogous to Case 1, so it also fails.
>
> Case 3: Suppose the fixed point of φ is in $\widehat{AB}$. Then $S^1 \backslash \widehat{AB}$ must be mapped onto $\widehat{A'B'}$. However, this creates a fixed point by the intermediate value theorem. So this case fails.

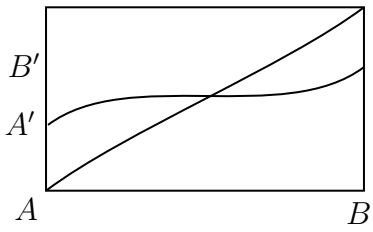

Case 4: Suppose the fixed point φ is in $\widehat{A'B'}$.This case is analogous to Case 3, so it also fails.

Thus φ cannot be parabolic. Recall that elliptic maps are simply rotations on S^1, by similar arguments to the parabolic cases, φ also cannot be elliptic. Therefore, φ must loxodromic. □

Proposition 5.2 Given the $\mathbb{H}^2$ realization of γ as in Figure 4, the corresponding loxodromic map φ has its repelling point in $\widehat{AB}$ and its attracting point in $\widehat{A'B'}$.

Proof: We again prove this by dynamics, by considering the different possibilities of combinations of the attracting point t and repelling point r.

Case 1: Let t, r both be in $\widehat{AA'}$ or both in $\widehat{BB'}$. Without loss of generality, suppose $t, r \in \widehat{AA'}$. Since φ is a loxodromic map, it's conjugate to a map that fixes 0 and ∞. This conjugate map must then have form $f(z) = (\frac{a}{d})z$. Use a map that sends $r \mapsto 0$ and $t \mapsto \infty$ while realizing this in upper-half plane. This is a neat set up because $(\mathbb{R} \cup \{\infty\}) - \{0, \infty\} = \mathbb{R}^- \cup \mathbb{R}^+$; the two components of S^1 created by a and r on S^1 correspond to $\mathbb{R}^-$ and $\mathbb{R}^+$. Notice since $ad = 1$, $(\frac{a}{d}) > 0$. So all f does is multiply them by a positive scalar.

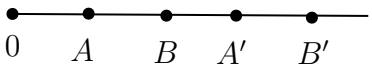

Notice that $A < B$ but $B' < A'$ which doesn't make sense if all we're doing is multiplying A and B by a positive number. Thus the cyclic order of orientation $ABB'A'$ doesn't make sense if f is supposed to preserve orientation. So this case fails.

Case 2: Using the same construction of the 2 components formed on S^1 by t and r in the previous case, we can argue the invalidity of cases where A, A' and B, B' are in different components, by recalling that all f does is multiply by a positive scalar. The following cases can be discarded.

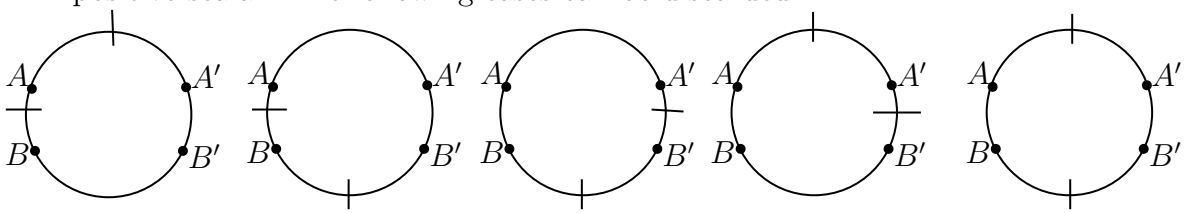

These five don't make sense because there is a pair of preimage/image that are in different components.

Case 3: Suppose t is in $\widehat{AB}$ and r is in $\widehat{A'B'}$. If t is sent to 0 and r is sent to ∞ in UHP, then the image of A is closer to repelling point than A. This contradicts the attracting/repelling notion of loxodromic maps. If t is sent to ∞ and r is sent to 0 in UHP, then likewise the image of A is being pulled in the direction of r instead of t, thus another contradiction. So this case fails.

Case 4: Suppose t, r are both in $\widehat{AB}$ or both in $\widehat{A'B'}$. Again without loss of generality, suppose $\widehat{AB}$ contains t, r as the argument for if they were in $\widehat{A'B'}$ is identical. Depending on the orientation of t and r in $\widehat{AB}$, either A is sent to a bigger number while B is sent to a smaller number in UHP or A is sent to a smaller number while B is sent to a larger number in UHP. Either case doesn't make sense since again f is multiplying by a positive scalar.

Therefore, the only possibility that stands is that $t \in \widehat{A'B'}$ and $r \in \widehat{AB}$. □

Proposition 5.3 A loxodromic map cannot have its cyclic order on S^1 be $AB'A'B$.

Proof: This construction will require the gluing to reverse orientability. Because polyhedra in $\mathbb{H}^3$ are orientable, reversing orientability in the $\mathbb{H}^2$ will disrupt the orientability of the polyhedron P. □

Thus far, we've shown that construction whose blueprints start and end like that of Figure 4, we have a loxodromic map whose repelling point is in $\widehat{AB}$ and attracting point is in $\widehat{A'B'}$. For this upcoming discussion, it would be to our benefit to include arbitrary vertices and geodesics.

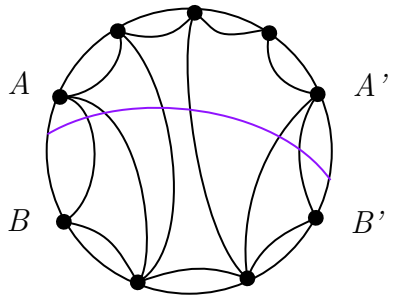

We can now consider the axis, the geodesic between the loxodromic map's attracting and repelling points. and make some observations about it. Before though, let us provide a lemma that will be most useful.

Lemma 5.4 For $x, y, a, b \in S^1$, $q(x, y) \cap q(a, b) \neq \varnothing$ if and only if a and b lie in different arcs of S^1 determined by x and y. Furthermore this intersection is unique.

Proof: ($\Rightarrow$) Assume $q(x, y) \cap q(a, b)$ intersect in $\mathbb{H}^2$. Also assume $q(x, y) \neq q(a, b)$. Use a Möbius map that sends $q(x, y)$ and $q(a, b)$ to UHP and makes $q(x, y)$ some bowed geodesic. If $q(a, b)$ is a vertical geodesic, then either a or b is on $\mathbb{R}$ and the

other must be ∞. If $q(a,b)$ also must intersect with a bowed geodesic, then either a or b must be contained within $x, y \in \mathbb{R}$. If $q(a,b)$ is a bowed geodesic and it intersects with $q(x,y)$, then $|c-c'| \leq r+r'$ where c, c' are centers of $q(x,y), q(a,b)$ and r, r' radii of $q(x,y), q(a,b)$ respectively. Then from this inequality we can claim that either a or b must be contained within $x, y \in \mathbb{R}$ and the other must be outside.

($\Leftarrow$) Assume $a \in \widehat{xy}$ and $b \notin \widehat{xy}$ and assume $q(x,y)$ is a bowed geodesic. If $q(a,b)$ is a vertical geodesic, then it clearly intersects with $q(x,y)$ since $a \in \widehat{x,y}$ and $b = \infty$. If $q(a,b)$ is a bowed geodesic, finding its center c' and radius r', its easy to check that $|c-c'| \leq r+r'$. Thus $q(a,b)$ must intersect $q(x,y)$. Also since geodesics can only intersect with one another in at most point, then it follows that the intersections discussed were unique. $\square$

Proposition 5.5 The loxodromic axis crosses the same edges as the given curve γ.

Proof: We repeatedly use Lemma 5.4 when we observe that the loxodromic axis, determined by ideal points x, y, separate the ideal vertices of each geodesic edge into different arcs of S^1 formed by x and y. $\square$

Fortunately for us, a well-known postulate from Euclidean geometry that remains true in hyperbolic geometry is that vertical angles are equal. Thus the vertical angles formed by $q(x,y)$, the purple geodesic, with its intersection of geodesic edges are equal. However, we'd like the vertical angles formed when we glue $q(A,B)$ and $q(A',B')$ with $q(x,y)$. That is, we'd like $\alpha = \beta$ as in the picture below.

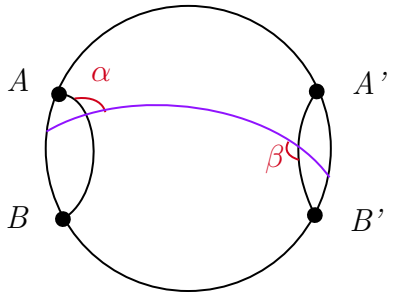

FIGURE 5. The set up for Proposition 5.6

Proposition 5.6 The angle α at the entrance point of φ is equal to the angle β at the exit point of φ.

Proof: Consider a point a on $q(A,B)$ and a point b on loxodromic axis such that $\measuredangle(a, \text{entrance point}, b) = \alpha$. By our loxodromic map φ, the entrance point is sent to the exit point. But since φ is a Möbius transformation, φ is both orientation-preserving and conformal. So $\measuredangle(\varphi(a), \text{exit point}, \varphi(b)) = \alpha$. But since this angle is vertical to β, then $\alpha = \beta$. $\square$

In this next comment, we use how 2 geodesics in $\mathbb{H}^2$ only intersect at a unique point unless the 2 geodesics were in fact the same geodesic. So the loxodromic axis touches each geodesic edge that doesn't have adjacent vertices once and only once. Moreover, these faces were drawn because these faces were the faces our curve γ travels on. If we denote the segment of the geodesic axis between the entrance and exiting point

$\overline{\gamma}$ as well give $\overline{\gamma}$ its natural loxodromic orientation, then it is clear that $\overline{\gamma}$ *follows* γ, meaning $\overline{\gamma}$ observes the face sequence in the same order as γ.

6. Turning angles

Lemma 3.3 was the stepping stone in the sense that we were required to first build up our comprehension of curves, namely those that correspond to loxodromic maps, so that we could start to think about how we implement Lemma 3.3 in such a way that instead of an inequality, we could construct an equality between dihedral and turning angles. We are particularly interested in loxodromic maps because it gives a voice in the conversation on angles due that its axis respects vertical angles for the gluing. We will now give a more intuitive name for the angles that are made with the loxodromic axis.

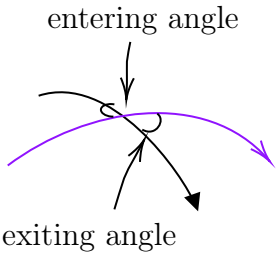

Let the purple geodesic be the loxodromic axis with the denoted orientation and the other geodesic be a geodesics edge. The angle at which the loxodromic axis enters at is called the 'entering angle', while the angle at which the loxodromic axis exits at is called the 'exiting angle'. We could also have chosen the other pair of vertical angles to the call the entering/exiting angles. We now consider γ to be the loxodromic axis. A thing to keep in mind in that in the realization $\mathbb{H}^2$ the loxodromic axis is indeed a geodesic, but on the polyhedron P in $\mathbb{H}^3$, the curve defined by the loxodromic axis is only locally a geodesic. It is a unique geodesic on each face of P it passes through.

Theorem 6.1 The turning angle τ at p of loxodromic axis $\overline{\gamma}$ for a corresponding closed polygonal curve on a convex ideal hyperbolic polyhedra P at each vertex satisfies

$$\cos(\tau) = \sin^2(\alpha)\cos(\pi - \delta) + \cos^2(\alpha)$$

where α is the entering/exiting angle at p and δ is the interior dihedral angles between the faces $\overline{\gamma}$ crosses between through p.

Proof: Consider the ball model and we're looking at where γ crosses from one face to another at an edge point p. Let δ be the interior dihedral angle between the faces in question. Suppose we use a Möbius map that sends p to 0, the center of the ball model. The geodesics of $\mathbb{H}^3$ that only cross through the center of the ball model are Euclidean planes. This forces the geodesics on both faces to become Euclidean line segments that pass through the center 0 of S^2 as in Figure 6. This is a convenient set up since we are more familiar with the geometry of Euclidean space than hyperbolic.

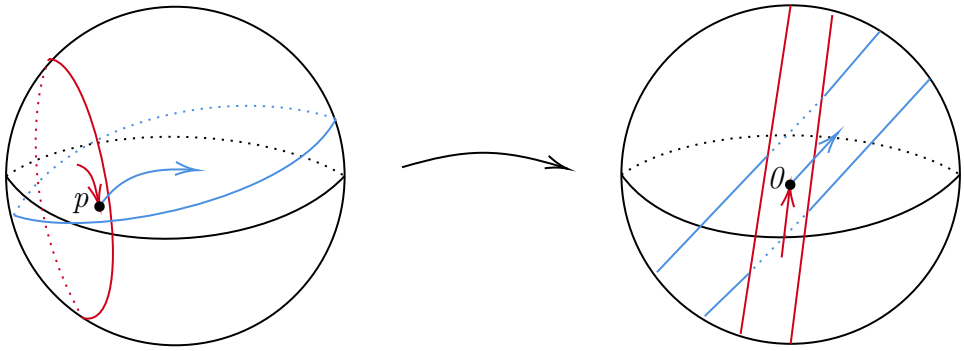

FIGURE 6. Mapping the ball model in such a way that makes the geodesics Euclidean planes

Being in the ball model for $\mathbb{H}^3$ is that we could simply rotate the ball in such a manner such that one of the Euclidean planes is the yz-plane if the ball is embedded in $\mathbb{R}^3$, all while preserving δ. Thus we can abandon the ball model and picture Euclidean planes in $\mathbb{R}^3$ as in Figure 7.

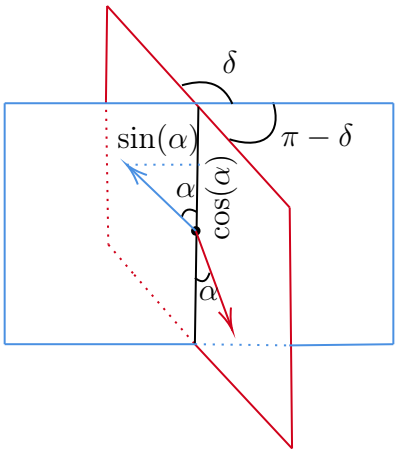

FIGURE 7. The yz-plane (blue) along with the other plane (red)

Let $\vec{v_1}$ be the vector in the yz-plane and $\vec{v_2}$ be the vector in the other plane. The vector $\vec{v_1}$ has no displacement in the x-direction since $\vec{v_1}$ lives on yz-plane. Since we oriented line of intersection between the planes to be the $z-$axis, the vertical displacement of $\vec{v_1}$ is simply $\cos(\alpha)$, while it's displacement in $y-$direction is $-\sin(\alpha)$. Therefore we get that

$$\vec{v_1} =< 0, -\sin(\alpha), \cos(\alpha) >$$

The vertical displacement of $\vec{v_2}$ will be $-\cos(\alpha)$. To figure out what the other 2 components of $v\vec{v_2}$ is a little trickier because it is not on the yz-plane. We must first project onto the horizontal plane that $\vec{v_2}$ meets at. Then we construct a right triangle whose hypotenuse is $\sin(\alpha)$ with its other angles being $\pi - \delta$ and δ. This immediately gives us that the displacement of $\vec{v_2}$ in the x-direction is $\sin(\alpha)\cos(\delta)$ and displacement in the y-direction is $\sin(\alpha)\sin(\delta)$. Thus $\vec{v_2}$ has the form

$$\vec{v_2} =< \sin(\alpha)\cos(\delta), \sin(\alpha)\sin(\delta), -\cos(\alpha) > .$$

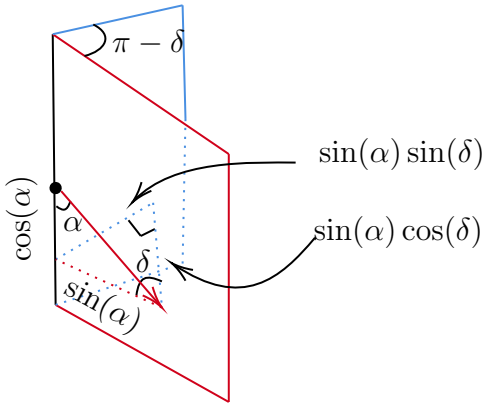

FIGURE 8. Projection onto a horizontal slice

If we were to take the dot product of $\vec{v_1}$ and $\vec{v_2}$, we would get the cosine of the angle between them. However what we want is the turning angle, the cosine of the supplementary angle. A way to get the turning angle to simply take the dot product of $-\vec{v_1}$ and $\vec{v_2}$. Notice we chose made $\vec{v_i}$ of unit length by construction.

$$-\vec{v_1} \cdot \vec{v_2} = \sin^2(\alpha)\sin(\delta) + \cos^2(\alpha)$$

$$\cos(\tau) = \sin^2(\alpha)\cos(\pi - \delta) + \cos^2(\alpha) \tag{6.1}$$

$$\cos(\tau) \geq \cos(\pi - \delta)$$

$$\tau \leq \pi - \delta \tag{6.2}$$

Equation 6.1 is the explicit formula that gives us the relationship turning angle τ, exterior dihedral angle $\pi - \delta$ and entering/exiting angle α $\square$.

Moreover, from Equation 6.1 we can deduce Rivin's upper bound condition, Inequality (6.2), of the turning angle.

7. Example

Let's try to come up with a closed curve that corresponds to a loxodromic map to see all of this in action. Suppose we have a tetrahedron P in the upper-half space model such that it has vertex at the point at infinity and the remaining vertices be the primitive third roots of unity. Figure 9 contains the tetrahedron and the curve for this example accompanied by the table.

$$\begin{array}{ccc} A = (\frac{-1}{2} + \frac{\sqrt{3}}{2}i, 0) & e_1 = (\frac{-1}{2}, \frac{\sqrt{3}}{2}) & e_4 = (\frac{-1}{2} + \frac{\sqrt{3}}{2}i, 1) \\ B = (\frac{-1}{2} - \frac{\sqrt{3}}{2}i, 0) & e_2 = (\frac{1}{4} - \frac{\sqrt{3}}{4}i, \frac{\sqrt{3}}{2}) & e_5 = (\frac{-1}{2} - \frac{\sqrt{3}}{2}i, 1) \\ C = (1, 0) & e_3 = (\frac{1}{4} + \frac{\sqrt{3}}{4}i, \frac{\sqrt{3}}{2}) & e_6 = (1, 1) \end{array}$$

Let's recall the procedure. We realize all the faces of P, which in this case is all of them, as copies of $\mathbb{H}^2$, glue the copies together, find the loxodromic map and it's axis. From then we can use the entering/exiting angle along with dihedral angles to find the total turning of the polygonal curve. Let the face sequence be $(ABD) \to (BCD) \to (ABC) \to (ACD) \to (ABD)$. First let's realize (ABD) as a

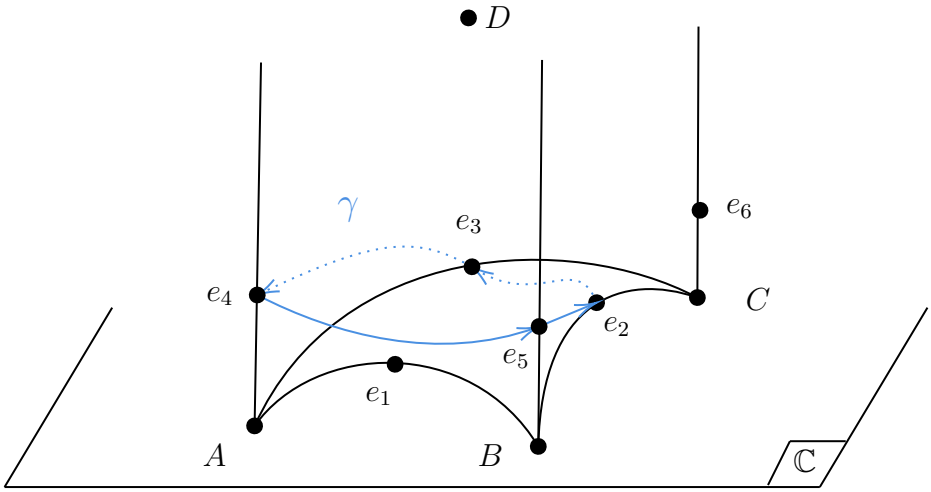

FIGURE 9. Ideal convex tetrahedron along with the closed curve γ

copy of $\mathbb{H}^2$.

Recall that the way we realize vertical planes as copies of $\mathbb{H}^2$ is by imagine the plane is just a copy of UHP. We can use an isometry that sends A to 0, B to $\sqrt{3}$ and fixes D. This isometry will send e_4 to i, e_5 to $\sqrt{3}+i$ and e_1 to $\frac{\sqrt{3}}{2}+\frac{\sqrt{3}}{2}i$. An easy way to send the UHP to the disk model is by mapping $0 \mapsto 1$, $\sqrt{3} \mapsto i$ and $\infty \mapsto -1$. The key to obtaining such a mapping was displayed in Proposition 2.1. Thus realization mapping is the following. Thus realization mapping is the following.

$$r_1(z) = \frac{-z+\sqrt{3}i}{z+\sqrt{3}i}$$

Recognizing that $1, i, -1$ correspond to A, BD respectively, we have the disk model

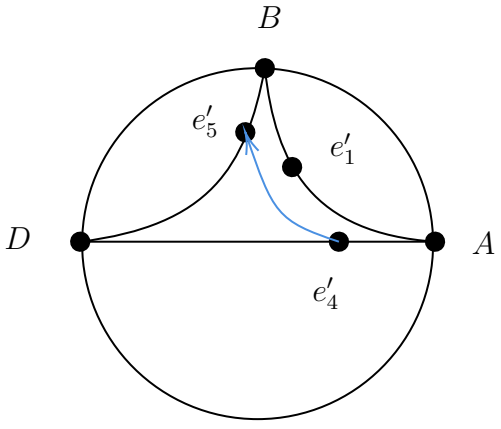

where

$$e_1' = \tfrac{1}{5}+\tfrac{2}{5}i \quad e_4' = 2-\sqrt{3} \quad e_5' = \tfrac{-3+18i}{21+6\sqrt{3}}$$

But this realization map isn't unique to (ABD). We can likewise use the same isometry to move faces (ACD) and (BCD) such that its vertices are $0, \sqrt{3}$ and ∞ and then apply r_1 to obtain identical copies of $\mathbb{H}^2$. Thus we get the faces (ACD) and (BCD).

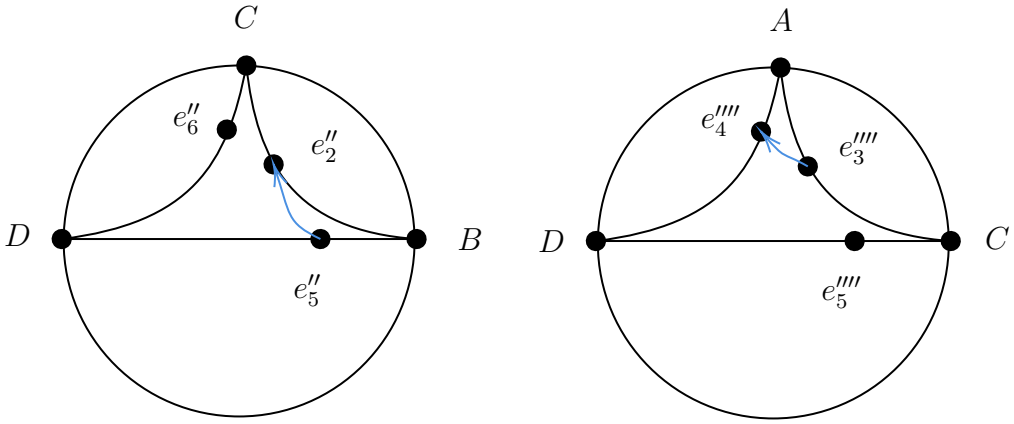

where

$$e_2'' = \tfrac{1}{5} + \tfrac{2}{5}i \quad e_5'' = 2 - \sqrt{3} \quad e_6'' = \tfrac{-3+18i}{21+6\sqrt{3}}$$
$$e_3'''' = \tfrac{1}{5} + \tfrac{2}{5}i \quad e_4'''' = \tfrac{-3+18i}{21+6\sqrt{3}} \quad e_5'''' = 2 - \sqrt{3}$$

To realize (ABC) as a copy of $\mathbb{H}^2$, we must stereographically project. Let's think of $\mathbb{C}$ as the $xy-$plane in $\mathbb{R}^3$. Since the vertices A, B, C determines the unit circle on $xy-$plane, the sphere containing them is the unit sphere. The face (ABC) is in fact lying on the unit sphere. Stereographically projecting the set of points within (ABC) through the south pole $(0, 0, -1)$, we get the realization

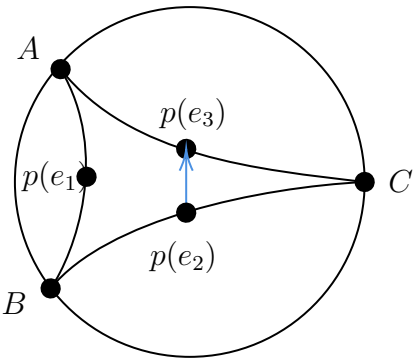

However as it stands, we will not be able to glue this copy of (ABC) to the others because the stereographic projection reversed orientation. An easy fix to this is to realize this face sitting in $\mathbb{C}$ and use complex conjugation, as it is an orientation-reversing isometry.

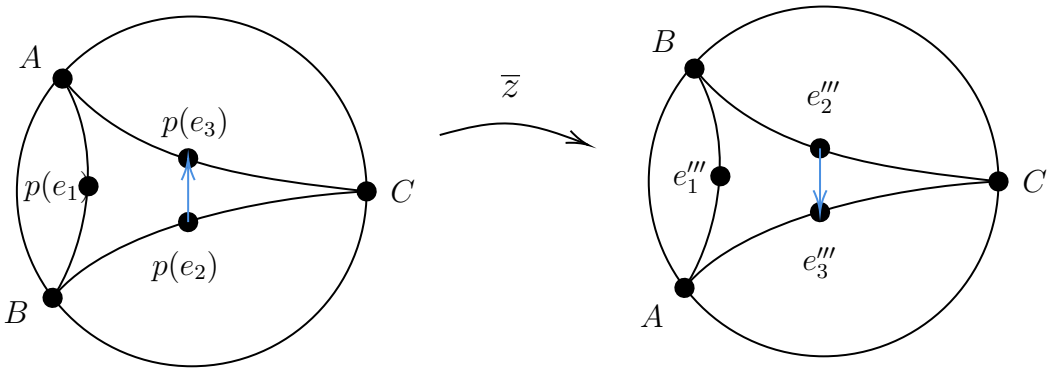

where

$$e_1''' = -2+\sqrt{3} \quad e_2''' = \tfrac{1+\sqrt{3}i}{4+2\sqrt{3}} \quad e_3''' = \tfrac{1-\sqrt{3}i}{4+2\sqrt{3}}$$

Now we have all of our faces of P as copies of $\mathbb{H}^2$. We can now begin gluing them altogether. To glue (CBD) onto (ABD), we need a map that sends $-1 \mapsto -1, 1 \mapsto i$ and $2-\sqrt{3} \mapsto \frac{-3+18i}{21+6\sqrt{3}}$. Since $\frac{-3+18i}{21+6\sqrt{3}}$ is an important edge point, call it a. Then the corresponding gluing map is

$$g_1(z) = \frac{(-1+2i)z-1}{z+(1+2i)}$$

This map g_1 sends $i \mapsto \frac{-3+4i}{5}$ and $\frac{1+2i}{5} \mapsto \frac{-1+2i}{3}$. Let $b = \frac{-1+2i}{3}$. We'd like to know $g_1(i)$ so we could draw the image of the triangle onto what we're calling the 'original copy', the face (ABD). Identify $g_1(i)$ by C on original copy. We'd like to know where g_1 sends $\frac{1+2i}{5}$ because the image is our next edge point. To glue (ABC) onto the original copy, we need a map that sends $\frac{-1+\sqrt{3}i}{2} \mapsto i$, $1 \mapsto \frac{-3+4i}{5}$ and $\frac{1+\sqrt{3}i}{4+2\sqrt{3}} \mapsto b$. The corresponding gluing map is

$$g_2(z) = \frac{(-12-5\sqrt{3}+i(3+4\sqrt{3}))z+(9+2\sqrt{3}+i(6+5\sqrt{3}))}{(6+5\sqrt{3}+i(9+2\sqrt{3}))z+(3+4\sqrt{3}+i(-12-5\sqrt{3}))}$$

This map g_2 sends $\frac{-1-\sqrt{3}i}{2} \mapsto \frac{-5+12i}{13}$ and $\frac{1-\sqrt{3}i}{4+2\sqrt{3}} \mapsto \frac{-2+4i}{5}$. Identify $g_2(\frac{-5+12i}{13})$ by A' on original copy and let $c = \frac{-2+4i}{5}$ since it will be the next gluing point. To glue (ACD) onto the original copy, we need a map that sends $i \mapsto \frac{-5+12i}{13}$, $1 \mapsto \frac{-3+4i}{5}$ and $\frac{1+2i}{5} \mapsto c$. The corresponding gluing map is

$$g_3(z) = \frac{(-4+5i)z+(6-i)}{(6+i)z+(-4-5i)}$$

This gluing map sends $-1 \mapsto \frac{-8+15i}{17}$ and $a \mapsto d = \frac{(-217-62\sqrt{3})+i(462+132\sqrt{3})}{523+160\sqrt{3}}$. Identify $g_4(-1)$ by D' on original copy. We have now glued all of our faces together, as shown in Figure 10 along with the curve γ.

To find the corresponding loxodromic map we care about, we just need to find the map that sends A' to A, D' to D and d to e_4'. Let this map be called φ. Thus, it takes on the form

$$\varphi(z) = \frac{-7z+(3-6i)}{(3+6i)z-7}$$

The form $\varphi(z)$ takes on agrees with Marden [Mar 23]. The loxodromic axis of φ is simply the geodesic between φ's fixed points, which are $z = \frac{-1+2i}{\sqrt{5}}, \frac{1-2i}{\sqrt{5}}$. Notice that since φ's fixed points are antipodal, then the loxodromic axis is a diameter of $\mathbb{H}^2$. Let Γ be the curve on the loxodromic axis of φ contained between the entrance and exiting point of loxodromic axis in the collection of faces. Let $(1), (2), (3), (4)$ be the intersection of Γ with geodesics $q(A,D), q(B,D), q(B,C), q(A',C)$ respectively. The point (1) is the entrance point and if we were to label a point (5), it would be the exiting point. We find the entering/exiting angles of Γ at (i) by finding tangent

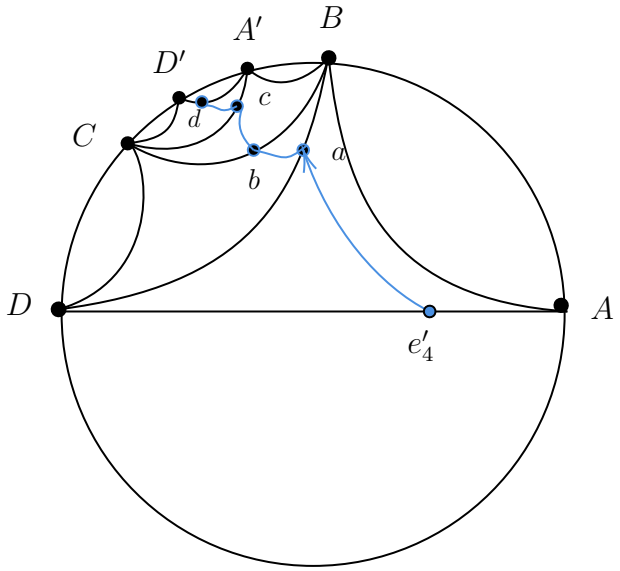

FIGURE 10. The curve γ on realized faces in $\mathbb{H}^2$

vectors of circles and using dot product between Γ and tangent vectors of circles at each corresponding point of intersection. Thus we can find the entering/exiting angles of Γ.

$$\cos\alpha_{(1)} = \tfrac{1}{\sqrt{5}} \quad \cos\alpha_{(2)} = \tfrac{-1}{\sqrt{5}} \quad \cos\alpha_{(3)} = \tfrac{1}{\sqrt{5}} \quad \cos\alpha_{(4)} = \tfrac{-1}{\sqrt{5}}$$

To apply equation (6.1), all that is left is find is dihedral angles of each face. If a tetrahedron has 3 ideal vertices on $\mathbb{C}$ and the other at ∞, then the dihedral angles are completely determined by the euclidean triangle formed by the ideal vertices on $\mathbb{C}$. Fortunately, $\triangle ABC$ form an equilateral triangle on $\mathbb{C}$. Angles formed by geodesics up in the space are preserved under stereographic projection, so we could work out angles on $\mathbb{C}$ in a euclidean-like manner. After calculations, we see that the exterior dihedral angle $\frac{2\pi}{3}$ remains constant over any pair of faces. Also notice that for any entering/exiting angle $\alpha_{(i)}$, $\cos\alpha_{(i)} = \frac{1}{5}$. So we see from equation (6.1),

$$\begin{aligned} \tau_{(i)} &= \arccos\left(\left(\tfrac{2}{\sqrt{5}}\right)^2 \cos\left(\tfrac{2\pi}{3}\right) + \left(\tfrac{1}{\sqrt{5}}\right)^2\right) \\ &= \arccos\left(\left(\tfrac{4}{5}\right)\left(\tfrac{-1}{2}\right) + \left(\tfrac{1}{5}\right)\right) \\ &= \arccos\left(\tfrac{-1}{5}\right) \end{aligned} \tag{7.1}$$

The total turning $\Sigma\tau_{(i)} = 4\arccos\left(\frac{-1}{5}\right)$ is greater than 2π, which agrees with Theorem 3.3.

8. FURTHER IDEAS

Speaking on the example, we saw that we begun sending one point to ∞ and the others to a specific set of points on $\mathbb{C}$. The example was catered such there was a lot of free symmetry given to us, primarily because the 3rd roots of unity on $\mathbb{C}$ form an equilateral triangle. Suppose however that we did not choose the 3rd roots of unity but a different set of points. Immediately, this changes the dihedral angles formed by the geodesic planes. However, where we send the 3 ideal vertices on $\mathbb{C}$

will also affect the edge points of γ. This consequently will affect the gluing maps g_i, which will in turn change the loxodromic map φ and result in a different curve of the loxodromic axis Γ. So changing the set of points acts in a waterfall effect in which it completely determines the things we are interested in. A well-known method to determine whether two tetrahedrons are isometric are whether their dihedral angles are the same. Since the 3 points on $\mathbb{C}$ determined our example and all we did was see how that calculation unravelled itself, it would be interesting if we could 'speed up' the process of obtaining Γ.

The reasoning to restrict our curves to basic face sequences is that then we'd have at our disposable a finite number of equivalence classes in the fundamental group of P. An initial question we asked was what equivalence class is the one that minimizes total turning/Γ length. Additionally, if there was a way to compare these two variables and seek out equivalence classes that relate the two in an interesting fashion. Since P has an infinite amount of equivalence classes, it was natural to restrict our curves to a specific class so that this problem could be tackled less colossally.

9. Acknowledgements

Firstly, I would like to thank UC Berkeley and the NSF for their support in giving me this opportunity to advance my career as a mathematician. I'd like to extend my sincere thanks to Franco Vargas Pallete, the program advisor, whose tenacious patience and guidance encouraged me to work hard. From my home institution at The College of New Jersey, I'd like to deeply thank Steffen Marcus, Cynthia Curtis and Andrew Clifford for sparking and fostering my interest in geometry and topology.

References

[1] Albert Marden. *Outer Circles: An Introduction Hyperbolic 3-manifolds*. Cambridge University Press. 2007

[2] Craig D. Hodgson, Igor Rivin. *A characterization of compact convex polyhedra in hyperbolic 3-space*. Inventiones mathematicae. Springer-Verlag. 1993

[3] Igor Rivin. *A Characterization of Ideal Polyhedra in Hyperbolic 3-Space*. Annals of Mathematics, Second Series Vol 143 No. 1. 1996

[4] William P. Thurston, Silvio Levy. *Three-Dimensional Geometry and Topology*. Princeton University Press. 1997

[5] Colin Adams, Robert Franzosa. *Introduction to Topology: Pure and Applied*. Pearson Prentice Hall. 2008

The College of New Jersey, department of mathematics, new jersey 08628
E-mail address: calvos1@tcnj.edu